

Nonlinear pulse propagation in a single- and a few-cycle regimes with Raman response

VIMLESH MISHRA and AJIT KUMAR*

Department of Physics, Indian Institute of Technology, Hauz Khas, New Delhi 110 016, India

Corresponding author. E-mail: ajitk@physics.iitd.ernet.in

MS received 16 February 2009; revised 1 February 2010; accepted 17 March 2010

Abstract. The propagation equation for a single- and a few-cycle pulses was derived in a cubic nonlinear medium including the Raman response. Using this equation, the propagation characteristics of a single- and a 4-cycle pulse, at $0.8\ \mu\text{m}$ wavelength, were studied numerically in one spatial dimension. It was shown that Raman term does influence the propagation characteristics of a single- as well as a few-cycle pulses by counteracting the self-steepening effect.

Keywords. Few-cycle pulse; nonlinear pulse propagation; Raman effect.

PACS Nos 42.50.Md; 42.65.Tg; 42.65.Sf

During the last few years, remarkable developments have taken place in experimental techniques for generating ultrashort pulses [1–4], which led to high-intensity optical pulses with pulse durations equal to one period of the optical cycle or less. Such ultrashort pulses have found applications [5–11] in diverse areas of physics and technology including nonlinear optical devices, all-optical communication, medical diagnostics and imaging, controlled manipulation of chemical reactions and bond formation, and coherent quantum control of microscopic dynamics. As a result, presently, there is a great deal of interest in the study of propagation characteristics of a single- and a few-cycle pulses in linear as well as nonlinear media.

In 1997, Brabec and Krausz [12] presented a novel model for nonlinear pulse propagation in the single-cycle regime in which they showed that, for such pulses, the concept of an envelope could be generalized in terms of the invariance of the central frequency of the pulse under a phase shift of the electric field. Based on this, they derived a nonlinear pulse evolution equation that represents a generalization of the well-known nonlinear Schroedinger equation. This model equation has been successfully used by several authors [13–17] in various studies including nonlinear propagation dynamics of an ultrashort pulse in a hollow waveguide [13], supercontinuum generation by filamentation of a few-cycle pulses [14], estimation of the critical power for self-focussing in bulk media and in hollow waveguides [15],

simulation of ultrabroadband light generation via self-channelling of a few-cycle pulses in a noble gas [16], generation of ultrashort pulses in a hollow-core fibre filled with a gas [17] etc.

In this work, we study the effect of the delayed nonlinear response (intrapulse Raman effect) on the propagation characteristics of a single- and a few-cycle pulse at 0.8 μm wavelength in a silica glass fibre within the slowly-evolving-wave approximation of Brabec and Krausz for a cubic medium. It is shown that Raman term does influence the propagation characteristics of a single- as well as a few-cycle pulses by counteracting self-steepening.

The nonlinear wave equation in a cubic medium, including the delayed third-order nonlinear response, can be written as

$$\begin{aligned} \left(\vec{\nabla}_{\perp}^2 + \frac{\partial^2}{\partial z^2} \right) E(\vec{r}, t) = & \frac{1}{c^2} \frac{\partial^2}{\partial t^2} \int_0^{\infty} \varepsilon(t') E(t - t') dt' \\ & + \frac{\sigma \chi^{(3)}}{c^2} \frac{\partial^2}{\partial t^2} ((\vec{E}(t) \cdot \vec{E}(t)) E(\vec{r}, t)) \\ & + \left(\frac{(1 - \sigma) \chi^{(3)}}{c^2} \right) \frac{\partial^2}{\partial t^2} \\ & \times \left(\vec{E}(t) \int_0^{\infty} g_R(t - t') (\vec{E}(t - t') \cdot \vec{E}(t - t')) dt' \right). \end{aligned} \quad (1)$$

In writing down the above equation, we have taken into account that the third-order nonlinear polarization consists of two terms:

$$\begin{aligned} \vec{p}_{\text{nl}} = \vec{p}_{\text{nl}}^{(1)} + \vec{p}_{\text{nl}}^{(2)} = & \sigma \varepsilon_0 \chi^{(3)} (\vec{E}(t) \cdot \vec{E}(t)) \vec{E}(t) \\ & + \varepsilon_0 \chi^{(3)} (1 - \sigma) \vec{E}(t) \int_{-\infty}^t g_R(t - t') (\vec{E}(t') \cdot \vec{E}(t')) dt', \end{aligned} \quad (2)$$

where σ is the fraction of the nonlinear polarization that is instantaneous (electronic) and $g_R(t)$ is the Raman response function. The value of σ is taken to be 0.7 [18,19]. Usually, the Raman response is approximated by damping oscillations associated with a single vibrational mode [18], resulting in a Lorentzian-shaped gain spectrum. This model uses three parameters (σ , τ_1 and τ_2) to provide the correct location and peak value of the dominant peak in the Raman gain spectrum. Note that the values of τ_1 and τ_2 are determined by curve fitting of the experimental data as done in ref. [18] for silica fibre. Because of its simplicity, this model is widely used and it explains the qualitative behaviour reasonably well. Under the above-mentioned assumption when only one vibrational mode, with linewidth $1/\tau_2$ and the eigenfrequency $1/\tau_1$, is important [19], the Raman response function is given by

$$g_R(t) = \frac{\tau_1^2 + \tau_2^2}{\tau_1 \tau_2^2} e^{-t/\tau_2} \sin\left(\frac{t}{\tau_1}\right), \quad (3)$$

where $\tau_1 = 12.2$ fs and $\tau_2 = 32$ fs. As shown by Brabec and Krausz [12], an envelope can be assigned to ultrashort pulses that contains at least one carrier cycle within

Nonlinear pulse propagation

their full-width at half-maximum (FWHM). Following that we represent the electric field of the pulse as

$$E(\vec{r}, t) = A(\vec{r}_\perp, z, t)e^{i(\beta_0 z - \omega_0 t)} + \text{c.c.}, \quad (4)$$

where β_0 is the propagation constant and ω_0 is the carrier frequency of the pulse.

Along with eqs (1)–(4), the Fourier transform of the first term on the right-hand side of eq. (1) with respect to the time coordinate, Taylor expansion of $k(\omega)$ around the carrier frequency ω_0 followed by an inverse Fourier transform yields

$$\begin{aligned} & (\vec{\nabla}_\perp^2 + \partial_z^2 + 2i\beta_0\partial_z - \beta_0^2)A(\vec{r}_\perp, z, t) \\ & + (\beta_0 + i\alpha_0/2 + i\beta^{(1)}\partial_t + \hat{D})^2 A(\vec{r}_\perp, z, t) \\ & = -\frac{\sigma\omega_0^2\chi^{(3)}}{c^2} \left[A \left(1 + \frac{i}{\omega_0}\partial_t\right)^2 |A|^2 + |A|^2 \left(1 + \frac{i}{\omega_0}\partial_t\right)^2 A + |A|^2 A \right] \\ & - \frac{(1-\sigma)\omega_0^2\chi^{(3)}}{c^2} \left(1 + \frac{i}{\omega_0}\partial_t\right)^2 \left(A(t) \int_0^\infty g_R(t') |A(t-t')|^2 dt' \right), \quad (5) \end{aligned}$$

where

$$\hat{D} = -\frac{\alpha_1}{2}\partial_t + \sum_{m=2}^{\infty} \frac{\beta^{(m)} + i\frac{\alpha^{(m)}}{2}}{m!} (i\partial_t)^m \quad (6)$$

$$\beta^{(m)} = \text{Re} \left[\left(\frac{\partial^m k}{\partial \omega^m} \right)_{\omega=\omega_0} \right], \quad (7)$$

$$\alpha^{(m)} = 2 \text{Im} \left[\left(\frac{\partial^m k}{\partial \omega^m} \right)_{\omega=\omega_0} \right]. \quad (8)$$

Taking into account that

$$\begin{aligned} \left(1 + \frac{i}{\omega_0}\frac{\partial}{\partial t}\right)^2 |A|^2 A &= A \left(1 + \frac{i}{\omega_0}\frac{\partial}{\partial t}\right)^2 |A|^2 \\ &+ |A|^2 \left(1 + \frac{i}{\omega_0}\frac{\partial}{\partial t}\right)^2 A + |A|^2 A \end{aligned} \quad (9)$$

and expanding $|A(t-t')|^2$ into a Taylor series around t' , we obtain

$$\begin{aligned} & (\vec{\nabla}_\perp^2 + \partial_z^2 + 2i\beta_0\partial_z - \beta_0^2)A(\vec{r}_\perp, z, t) \\ & + (\beta_0 + i\alpha_0/2 + i\beta^{(1)}\partial_t + \hat{D})^2 A(\vec{r}_\perp, z, t) \\ & = -\frac{\sigma\omega_0^2\chi^{(3)}}{c^2} \left[\left(1 + \frac{i}{\omega_0}\partial_t\right)^2 |A|^2 A \right] - \frac{(1-\sigma)\omega_0^2\chi^{(3)}}{c^2} \left(1 + \frac{i}{\omega_0}\partial_t\right)^2, \end{aligned}$$

$$\begin{aligned}
 & \left(|A(t)|^2 A(t) \int_0^\infty g_R(t') dt' - A(t) \frac{\partial |A|^2}{\partial t} \int_0^\infty t' g_R(t') dt' \right) \\
 &= -\frac{\omega_0^2 \chi^{(3)}}{c^2} \left[\left(1 + \frac{i}{\omega_0} \partial_t \right)^2 |A|^2 A \right] \\
 & \quad + \frac{(1-\sigma)\omega_0^2 \chi^{(3)}}{c^2} T_R \left(1 + \frac{i}{\omega_0} \partial_t \right)^2 \left(A \frac{\partial |A|^2}{\partial t} \right). \tag{10}
 \end{aligned}$$

Let us go over to the moving frame through the new variables

$$\tau = t - \beta^{(1)} z = t - \frac{z}{v_g}, \quad \xi = z. \tag{11}$$

As a result

$$\partial_z = \partial_\xi A - \beta^{(1)} \partial_\tau A \tag{12}$$

$$\partial_z^2 = \partial_\xi^2 A - 2\beta^{(1)} \partial_{\xi\tau}^2 A + \beta^{(1)2} \partial_\tau^2. \tag{13}$$

Dividing throughout by $2i\beta_0$ and taking into account the above expressions and the fact that $[\partial_\tau, \hat{D}] = 0$, we arrive at

$$\begin{aligned}
 & \partial_\xi A - \frac{\beta_0}{2i} A + \frac{1}{2i\beta_0} \partial_\xi^2 A - \beta^{(1)} \partial_\tau A - \frac{\beta^{(1)}}{i\beta_0} \partial_{\xi\tau}^2 A + \frac{\beta^{(1)2}}{2i\beta_0} \partial_\tau^2 A \\
 & + \frac{1}{2i\beta_0} \vec{\nabla}_\perp^2 A + \frac{\beta_0}{2i} A - \frac{\alpha_0^2}{8i\beta_0} A + \frac{\alpha_0}{2} A - \frac{\beta^{(1)2}}{2i\beta_0} \partial_\tau^2 A + \frac{\beta^{(1)}}{\beta_0} \partial_\tau (\hat{D} A) \\
 & + \beta^{(1)} \partial_\tau A - i \hat{D} A - \frac{\alpha_0 \beta^{(1)}}{2i\beta_0} \partial_\tau A + \frac{\alpha_0}{2\beta_0} \hat{D} A + \frac{1}{2i\beta_0} \hat{D}^2 A \\
 & - \frac{\omega_0^2 \chi^{(3)}}{2i\beta_0 c^2} \left[\left(1 + \frac{i}{\omega_0} \partial_t \right)^2 |A|^2 A \right] \\
 & + \frac{(1-\sigma)\omega_0^2 \chi^{(3)}}{2i\beta_0 c^2} T_R \left(1 + \frac{i}{\omega_0} \partial_t \right)^2 \left(A \frac{\partial |A|^2}{\partial \tau} \right) = 0. \tag{14}
 \end{aligned}$$

Taking into account that

$$\omega_0^2 = \frac{\beta_0^2 c^2}{n_0^2}, \quad \chi^{(3)} = \frac{8n_0 n_2}{3} \tag{15}$$

$$\frac{\omega_0^2 \chi^{(3)}}{2i\beta_0 c^2} = \frac{4\beta_0 n_2}{3in_0}, \tag{16}$$

where n_0 and n_2 are the linear refractive index and the Kerr coefficient respectively of the medium. Further, cancelling the terms in the above equation and adding and subtracting the term Ω

$$\Omega = \frac{i}{\omega_0} \partial_\tau \left(\partial_\xi + \frac{\alpha_0}{2} - i\hat{D} \right) A \quad (17)$$

we obtain

$$\begin{aligned} & \left(1 + \frac{i}{\omega_0} \partial_\tau \right) \left(\partial_\xi + \frac{\alpha_0}{2} - i\hat{D} \right) A \\ & + \frac{4\beta_0 n_2}{3in_0} \left(1 + \frac{i}{\omega_0} \partial_\tau \right)^2 |A|^2 A + \frac{1}{2i\beta_0} \vec{\nabla}_\perp^2 A \\ & = i \left(\frac{\beta_0 - \omega_0 \beta^{(1)}}{\omega_0 \beta_0} \right) \partial_\tau \left(\partial_\xi + \frac{\alpha_0}{2} - i\hat{D} \right) A \\ & - \frac{1}{2i\beta_0} \left(\partial_\xi^2 - \frac{\alpha_0^2}{4} + i\alpha_0 \hat{D} + \hat{D}^2 \right) A \\ & + \frac{4(1-\sigma)\beta_0 n_2}{3in_0} T_R \left(1 + \frac{i}{\omega_0} \partial_t \right)^2 \left(A \frac{\partial |A|^2}{\partial \tau} \right). \end{aligned} \quad (18)$$

If the relations

$$\left| \frac{\partial A}{\partial \xi} \right| \ll \beta_0 |A|, \quad \left| \frac{\partial A}{\partial \tau} \right| \ll \omega_0 |A|, \quad (19)$$

$$\left| \frac{\beta_0 - \omega_0 \beta^{(1)}}{\omega_0 \beta_0} \right| \ll 1, \quad (20)$$

representing the slowly varying wave approximation of Brabec and Krausz [12] hold good, then all the terms on the right-hand side except the last term are much smaller than the terms on the left-hand side of eq. (23) and hence can be neglected. The resulting equation is then

$$\begin{aligned} & \left(1 + \frac{i}{\omega_0} \partial_\tau \right) \left(\partial_\xi + \frac{\alpha_0}{2} - i\hat{D} \right) A \\ & + \frac{1}{2i\beta_0} \vec{\nabla}_\perp^2 A + \frac{4\beta_0 n_2}{3in_0} \left(1 + \frac{i}{\omega_0} \partial_\tau \right)^2 |A|^2 A \\ & = \frac{4(1-\sigma)\beta_0 n_2}{3in_0} T_R \left(1 + \frac{i}{\omega_0} \partial_t \right)^2 \left(A \frac{\partial |A|^2}{\partial \tau} \right). \end{aligned} \quad (21)$$

If we neglect damping and act on the equation from left by the operator

$$\left(1 + \frac{i}{\omega_0} \partial_\tau \right)^{-1} \quad (22)$$

we obtain Brabec and Krausz equation with Raman term

$$\left(\partial_\xi - i\hat{D} \right) A + \frac{1}{2i\beta_0} \left(1 + \frac{i}{\omega_0} \partial_\tau \right)^{-1} \vec{\nabla}_\perp^2 A$$

$$\begin{aligned}
 & + \frac{4\beta_0 n_2}{3in_0} \left(1 + \frac{i}{\omega_0} \partial_\tau\right) |A|^2 A \\
 & = \frac{4(1-\sigma)\beta_0 n_2}{3in_0} T_R \left(1 + \frac{i}{\omega_0} \partial_t\right) \left(A \frac{\partial |A|^2}{\partial \tau}\right). \tag{23}
 \end{aligned}$$

If the dispersion operator is given by $\hat{D} = (-\beta^{(2)}/2)(\partial^2/\partial\tau^2)$ and we multiply throughout by i , then we obtain the evolution equation as

$$\begin{aligned}
 & i \frac{\partial A}{\partial \xi} - \frac{\beta^{(2)}}{2} \frac{\partial^2}{\partial \tau^2} A + \frac{1}{2\beta_0} \left(1 + \frac{i}{\omega_0} \partial_\tau\right)^{-1} \vec{\nabla}_\perp^2 A \\
 & + \frac{4\beta_0 n_2}{3n_0} \left(1 + \frac{i}{\omega_0} \partial_\tau\right) |A|^2 A \\
 & - \frac{4(1-\sigma)\beta_0 n_2}{3n_0} T_R \left(1 + \frac{i}{\omega_0} \partial_t\right) \left(A \frac{\partial |A|^2}{\partial \tau}\right) = 0. \tag{24}
 \end{aligned}$$

The above partial differential equation describes pulse propagation in a cubic non-linear medium with Raman response in the framework of slowly evolving wave approximation of Brabec and Krausz.

1. Numerical results for one-dimensional propagation

For pulse propagation in one spatial dimension, say, in a silica glass fibre, the above equation reduces to

$$\begin{aligned}
 & i \frac{\partial A}{\partial \xi} - \frac{\beta^{(2)}}{2} \frac{\partial^2}{\partial \tau^2} A + \frac{4\beta_0 n_2}{3n_0} \left(1 + \frac{i}{\omega_0} \partial_\tau\right) |A|^2 A \\
 & - \frac{4(1-\sigma)\beta_0 n_2}{3n_0} T_R \left(1 + \frac{i}{\omega_0} \partial_t\right) \left(A \frac{\partial |A|^2}{\partial \tau}\right) = 0. \tag{25}
 \end{aligned}$$

We have numerically solved this equation for a single- and a four-cycle pulses at $0.8 \mu\text{m}$ wavelength for different regimes of propagation: without dispersion and Raman response, with dispersion but without Raman response and with dispersion and Raman response, in order to bring out the influence of the dispersive and Raman terms on pulse propagation described by the Brabec-Krausz model.

The input pulse is taken to be of hyperbolic secant form:

$$A = \text{sech}(1.76t/\tau_p), \tag{26}$$

where τ_p is the pulse width. The calculations have been carried out with the following parameters: $n_0 = 1.45$, $n_2 = 3 \times 10^{-16} \text{ cm}^2/\text{W}$, $I = 4 \times 10^{13} \text{ W}/\text{cm}^2$, $\omega_0 = 2.3483 \times 10^{15} \text{ rad/s}$, the speed of light $c = 2.9979 \times 10^8 \text{ m/s}$, dispersion parameter $\beta^{(2)} = 0.03923 \text{ fs}^2/\mu\text{m}$, Raman response time $T_r = 3 \text{ fs}$, $\sigma = 0.7$ and $\tau_p = 2.67 \text{ fs}$ which corresponds to a single optical cycle at $0.8 \mu\text{m}$ wavelength.

In figures 1a-c we have the dimensionless electric, $\bar{E}(\bar{t})$ field of a single-cycle pulse as a function of the dimensionless time \bar{t} for propagation without dispersion

Nonlinear pulse propagation

and Raman term, with dispersion but without delayed Raman response and with dispersion and the Raman response, respectively. The plots are for $14\text{ }\mu\text{m}$ of propagation distance which is very close to the characteristic distance of self-steepening $z_s \equiv 14.45\text{ }\mu\text{m}$. As we see in figure 1a the pulse has undergone considerable self-steepening, as expected, with the centre of the pulse shifted towards the trailing edge. Figure 1b shows that dispersion partially compensates for steepening of the wavefront. However, we can see that the pulse is still dominated by self-steepening. In figure 1c the effect of the delayed Raman response, in helping the pulse to tend to regain its initial symmetric shape, is clearly visible. Physically, when the spectral width exceeds a few terahertz, the high-frequency components of the pulse start pumping the lower-frequency components of the same pulse. This results in a gradual shift of the pulse spectrum towards longer wavelengths (lower frequencies) as the pulse propagates inside the medium (fibre). On the other hand, self-steepening

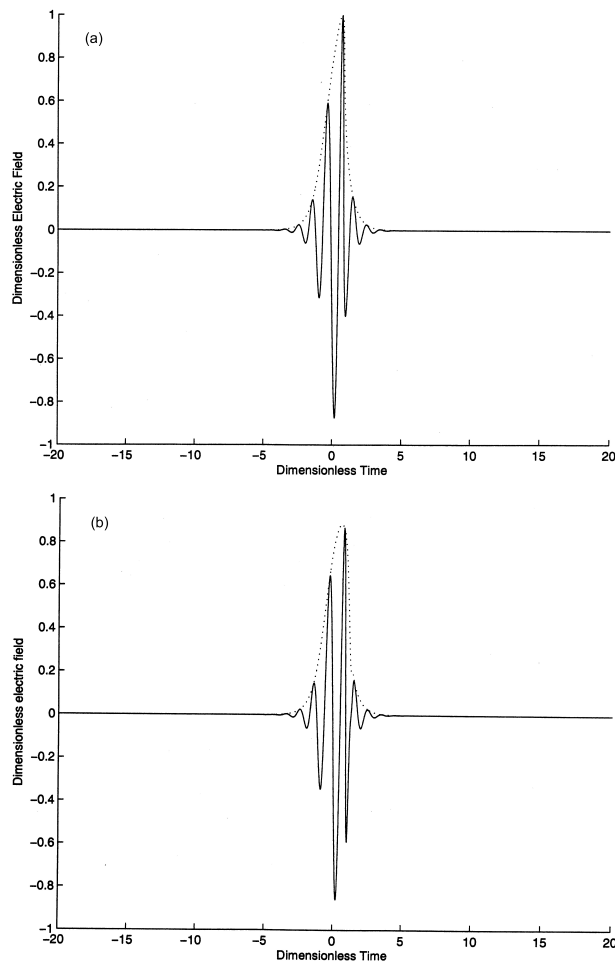


Figure 1(a) and (b).

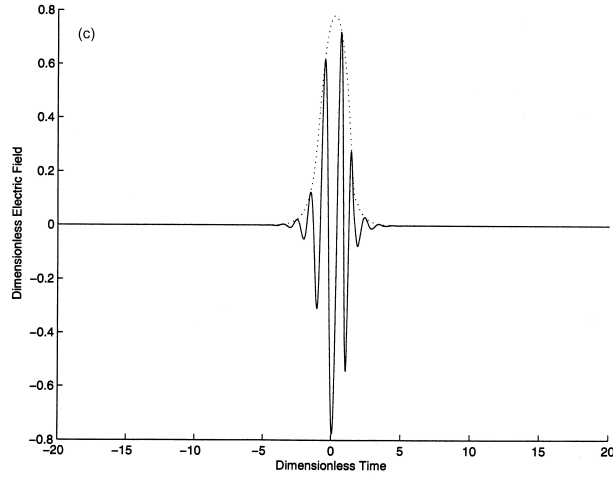


Figure 1. (a) The dimensionless electric field \bar{E} of a single-cycle pulse, at $0.8 \mu\text{m}$ wavelength, as a function of the dimensionless time \bar{t} , after $14 \mu\text{m}$ of propagation, for $n_2 = 3 \times 10^{-16} \text{ cm}^2/\text{W}$, $I = 4 \times 10^{13} \text{ W/cm}^2$, $\beta^{(2)} = 0$ and $\sigma = 1$. (b) The dimensionless electric field \bar{E} of a single-cycle pulse, at $0.8 \mu\text{m}$ wavelength, as a function of the dimensionless time \bar{t} , after $14 \mu\text{m}$ of propagation, for $n_2 = 3 \times 10^{-16} \text{ cm}^2/\text{W}$, $I = 4 \times 10^{13} \text{ W/cm}^2$, $\beta^{(2)} = 0.03923 \text{ fs}^2/\mu\text{m}$ and $\sigma = 1$. (c) The dimensionless electric field \bar{E} of a single-cycle pulse, at $0.8 \mu\text{m}$ wavelength, as a function of the dimensionless time \bar{t} , after $14 \mu\text{m}$ of propagation, for $n_2 = 3 \times 10^{-16} \text{ cm}^2/\text{W}$, $I = 4 \times 10^{13} \text{ W/cm}^2$, $\beta^{(2)} = 0.03923 \text{ fs}^2/\mu\text{m}$, $T_r = 3 \text{ fs}$, and $\sigma = 0.7$.

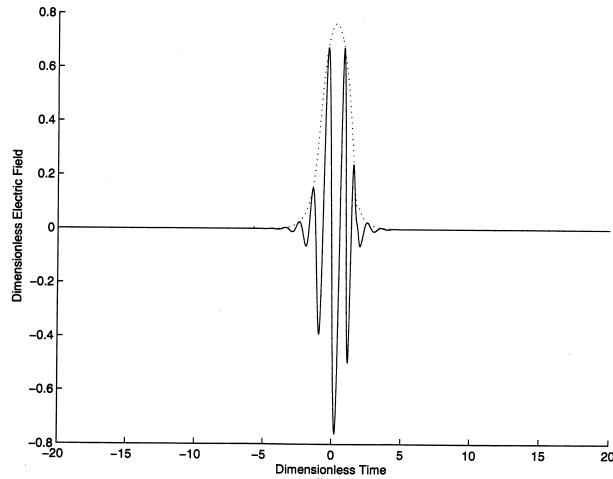


Figure 2. The dimensionless electric field \bar{E} of a single-cycle pulse, at $0.8 \mu\text{m}$ wavelength, as a function of the dimensionless time \bar{t} , after $16.3 \mu\text{m}$ of propagation, for $n_2 = 3 \times 10^{-16} \text{ cm}^2/\text{W}$, $I = 4 \times 10^{13} \text{ W/cm}^2$, $\beta^{(2)} = 0.03923 \text{ fs}^2/\mu\text{m}$, $T_r = 3 \text{ fs}$ and $\sigma = 0.7$.

Nonlinear pulse propagation

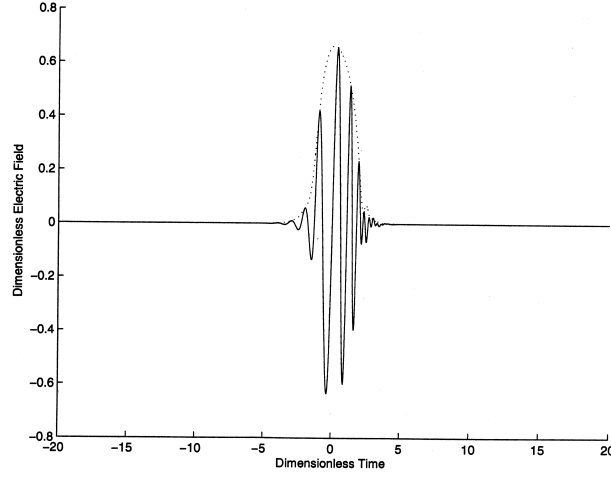


Figure 3. The dimensionless electric field \bar{E} of a single-cycle pulse, at $0.8 \mu\text{m}$ wavelength, as a function of the dimensionless time \bar{t} , after $32.6 \mu\text{m}$ of propagation, for $n_2 = 3 \times 10^{-16} \text{ cm}^2/\text{W}$, $I = 4 \times 10^{13} \text{ W/cm}^2$, $\beta^{(2)} = 0.03923 \text{ fs}^2/\mu\text{m}$, $T_r = 3 \text{ fs}$ and $\sigma = 0.7$.

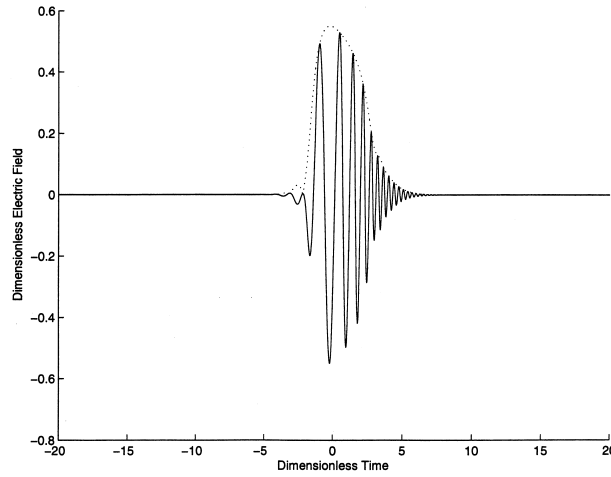


Figure 4. The dimensionless electric field \bar{E} of a single-cycle pulse, at $0.8 \mu\text{m}$ wavelength, as a function of the dimensionless time \bar{t} , after $65.2 \mu\text{m}$ of propagation, for $n_2 = 3 \times 10^{-16} \text{ cm}^2/\text{W}$, $I = 4 \times 10^{13} \text{ W/cm}^2$, $\beta^{(2)} = 0.03923 \text{ fs}^2/\mu\text{m}$, $T_r = 3 \text{ fs}$ and $\sigma = 0.7$.

effect leads to a frequency shift toward higher frequencies, in the trailing edge and toward lower frequencies in the leading edge. Since dispersion is positive ($\beta^{(2)} > 0$), the leading edge moves faster than the trailing edge and imparts an asymmetry to the pulse by steepening the trailing edge. Since the frequency shifts due to intra-pulse Raman effect and that due to self-steepening are opposite to each other the

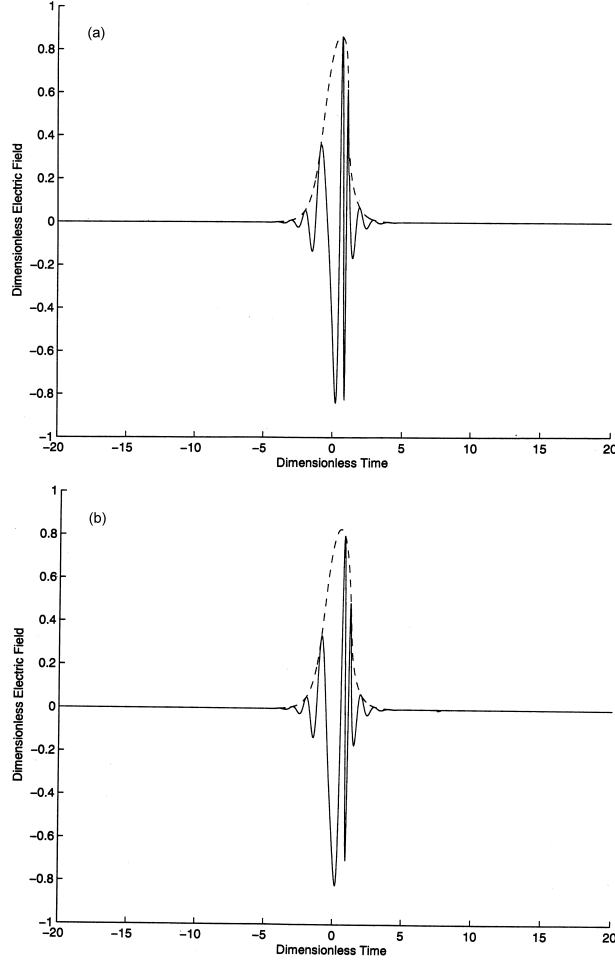


Figure 5. (a) The dimensionless electric field \bar{E} of a 4-cycle pulse, at $0.8 \mu\text{m}$ wavelength, as a function of the dimensionless time \bar{t} , after $57.37 \mu\text{m}$ of propagation without the Raman term, for $n_2 = 3 \times 10^{-16} \text{ cm}^2/\text{W}$, $I = 4 \times 10^{13} \text{ W/cm}^2$, $\beta^{(2)} = 0.03923 \text{ fs}^2/\mu\text{m}$, $T_r = 3 \text{ fs}$ and $\sigma = 0.7$. (b) The dimensionless electric field \bar{E} of a 4-cycle pulse, at $0.8 \mu\text{m}$ wavelength, as a function of the dimensionless time \bar{t} , after $78.24 \mu\text{m}$ of propagation with Raman term, for $n_2 = 3 \times 10^{-16} \text{ cm}^2/\text{W}$, $I = 4 \times 10^{13} \text{ W/cm}^2$, $\beta^{(2)} = 0.03923 \text{ fs}^2/\mu\text{m}$, $T_r = 3 \text{ fs}$ and $\sigma = 0.7$.

asymmetry of the pulse, introduced by self-steepening, gets neutralized and the symmetry of the pulse shape is restored.

In figures 2 and 3 we have the plots of the dimensionless electric field of the pulse as a function of the dimensionless time after 16.3 and $32.6 \mu\text{m}$ of propagation, respectively. As we see, in figure 2, the pulse has broadened due to dispersion but the pulse shape has regained its initial symmetry after the pulse has gone past the characteristic self-steepening length. However, for longer propagation distance

(figure 3) dispersive effects start dominating leading to the generation of oscillatory structure in the trailing edge of the pulse. The character of propagation remains the same for still longer distances with a difference that more and more cycles are generated as the pulse travels farther and farther away from the characteristic self-steepening length. This can be seen in figure 4 where we have the plot of the pulse electric field after $65.2 \mu\text{m}$ of propagation.

In figure 5a we have the plot of the dimensionless electric field for a 10.68 fs pulse, corresponding to four cycles at $0.8 \mu\text{m}$ wavelength, after $57.37 \mu\text{m}$ of propagation under the simultaneous influence of dispersion and self-steepening only. Note that for the given case the characteristic length equals $57.8 \mu\text{m}$. As we see, the propagation is dominated by the self-steepening effect which is counteracted by dispersive effects to some extent. In figure 5b we have the same plot with Raman term included in the evolution equation. We clearly see that the asymmetry caused by self-steepening has been further lessened by Raman effect. The same holds good for larger distances of propagation.

2. Conclusion

We have studied the influence of intrapulse Raman effect on the propagation characteristics of a single- and a few-cycle pulse in the framework of Barbec and Krausz model based on slowly varying wave approximation. Our study shows that the Raman term counteracts the self-steepening effect not only for a single-cycle pulse but also for a few-cycle pulse. Overall, the dynamics of the pulse is dominated by the self-steepening effect and dispersion. For propagation distances much larger than the characteristic self-steepening length, dispersion dominates and generates dense oscillatory structure in the trailing edge of the pulse.

Acknowledgement

Vimlesh Kumar Mishra acknowledges the financial support of the University Grants Commission, Government of India, through the Junior Research Fellowship Programme.

References

- [1] E Goulielmakis, M Uiberacker, R Kienberger, A Baltuska, V Yakovlev, A Scrinzi, Th Westerwalbesloh, U Kleineberg, U Heinzmann, M Drescher and F Krausz, *Science* **305**, 1267 (2004)
- [2] Rodrigo Lopez-Martens, Katalin Varj, Per Johnsson, Johan Mauritsson, Yann Mairesse, Pascal Salieres, Mette B Gaarde, Kenneth J Schafer, Anders Persson, Sune Svanberg, Claes-Gran Wahlstrm and Anne L'Huillier, *Phys. Rev. Lett.* **94**, 033001 (2005)
- [3] G D Tsakiris, K Eidmann, J Meyer-ter-Vehn and F Krausz, *New J. Phys.* **8**, 19 (2006)
- [4] M B Johnston, D M Whittaker, A Dowd, A G Davies, E H Linfield, X Li and D A Ritchie, *Opt. Lett.* **27**, 1935 (2002)

- [5] A Scrinzi, M Yu Ivanov, R Kienberger and D M Villeneuve, *J. Phys.* **B39**, R1 (2004)
- [6] M Drescher and F Krausz, *J. Phys.* **B38**, S727 (2005)
- [7] T Brabec and F Krausz, *Rev. Mod. Phys.* **72**, 545 (2000)
- [8] G P Agrawal, *Nonlinear fiber optics* (Academic Press, Boston, 1995)
- [9] A Baltus Caronka, Th Udem, M Uiberacker, M Hentschel, E Goulielmakis, Ch Gohle, R Holzwarth, V S Yakovlev, A Scrinzi, T W Hnsch and F Krausz, *Nature (London)* **421**, 611 (2003)
- [10] P Corkum, *Nature (London)* **403**, 845 (2000)
- [11] T Misgeld and M Kerschensteiner, *Nature Rev. (Neurosci.)* **7**, 463 (2006)
- [12] T Brabec and F Krausz, *Phys. Rev. Lett.* **78**, 3282 (1997)
- [13] D Homoelle and Alexander L Gaeta, *Opt. Lett.* **25**, 761 (2000)
- [14] S A Trushin, K Kosma, W Fu and W E Schmid, *Opt. Lett.* **32**, 2432 (2007)
- [15] G Fibich and A L Gaeta, *Opt. Lett.* **25**, 335 (2000)
- [16] E Goulielmakis, S Koehler, B Reiter, M Schultze, A J Verhoef, E E Serebryannikov, A M Zheltikov and F Krausz, *Opt. Lett.* **33**, 1407 (2008)
- [17] M Nurhuda, A Suda, M Hatayama, K Nagasaka and K Midorikawa, *Phys. Rev.* **A66**, 023811 (2002)
- [18] K J Blow and D Wood, *IEEE J. Quantum Electron.* **QE-25**, 2665 (1989)
- [19] J H B Nijhof, H A Ferverda and B J Hoenders, *Pure Appl. Opt.* **4**, 199 (1995)